2D and 3D lanthanide coordination polymers constructed from benzimidazole-5,6-dicarboxylic acid and sulfate bridged secondary building units†

Zhao-Xi Wang,*[a] Qiong-Fang Wu,[a] Hong-Jiang Liu,[a] Min Shao,[b] Hong-Ping Xiao[c] and Ming-Xing Li*[a]

Received 2nd June 2009, Accepted 31st October 2009
First published as an Advance Article on the web 1st December 2009
DOI: 10.1039/b910701k

Hydrothermal reaction of $Ln(NO_3)\cdot 6H_2O$ with benzimidazole-5,6-dicarboxylic acid (H_3bidc) and KSCN afforded a series of new two- and three-dimensional coordination polymers, namely $[Ln_2(Hbidc)_2(SO_4)(H_2O)_3]_n$ (Ln = La (**1**), Pr (**2**), Sm (**3**), Gd (**4**)) and $[Ln_4(Hbidc)_4(SO_4)_2]_n\cdot 2nH_2O$ (Ln = Eu (**5**), Tb (**6**), Dy (**7**), Er (**8**)). The sulfates were *in situ* generated by catalytic oxidation of KSCN. These complexes were characterized by single crystal X-ray diffraction, IR spectroscopy, thermal analysis, fluorescent spectra and magnetic measurements. Complexes **1–4** are isomorphous and comprise a 2D network based upon planar tetranuclear lanthanide secondary building units. The 2D layers extend to a 3D framework by π–π stacking between imidazole rings and hydrogen bonding interactions. The complexes **5–8** are also isomorphous and have similar 3D frameworks fabricated through $Hbidc^{2-}$ and SO_4^{2-} bridging dinuclear lanthanide secondary building units, and the guest water molecules are trapped in the lattice. The luminescent properties of complexes **5** and **6** exhibit characteristic europium and terbium luminescence, while **4** involves ligand-to-metal charge transfer. The magnetic properties of four complexes were also investigated.

Introduction

Recently, design and construction of coordination polymers based on secondary building units (SBUs) have attracted more attention in the field of crystal engineering due to their novel and diverse topologies and potential applications in host–guest chemistry, catalysis, electrical conductivity, magnetism, porosity, and optical properties.[1] Because the SBUs have various building-block geometries, which can show different spatial configurations, a variety of interesting topologies can be found in the crystal structure of their complexes.[2] In literatures, most of complexes constructed by SBUs contain transition metals, or both lanthanide and transition metal ions.[3] Compared to first-row transition metals, lanthanide metal ions have larger coordinate sphere and more flexible coordinate geometry.[4] These characteristics give rise to the lanthanide polymers exhibiting very complicated topologies. The construction of lanthanide coordination polymers based on SBUs has been much less developed so far.[4b,5]

As we know, carboxylate ligands are favorite candidates for constructing polymers with SBUs due to their diverse binding modes.[6] In the carboxylate family, *N*-heterocyclic carboxylic acids have been frequently used as bridging ligands between metal ions, forming coordination polymers with interesting topologies and functional properties.[7] For example, Zhang *et al.* used benzotriazole-5-carboxylate as a bridging ligand to construct a novel 3D metal–organic framework with "sra" topology.[8] Benzimidazole-5,6-dicarboxylic acid (H_3bidc), as a multidentate rigid ligand, has multiple coordinate sites involving two imidazole nitrogen atoms and four carboxylate oxygen atoms. It has three different abstractable hydrogens and is a good bridging ligand for constructing multi-dimensional polymers.[9] Up to now, a few cases of H_3bidc coordination complexes with a single metal center have been presented,[10] but none of them were constructed from secondary building units.

Anions, such as phosphates, halides and sulfate, as bridges incorporated in inorganic lattices and organic–inorganic complexes have been well documented.[11] They are not only used as a passive constituent but also as a contributor to increase complexity and exert a synergistic influence in the structural control for self-assembly.[12] Sulfate, a versatile auxiliary bridge, plays an important role in construction of coordination polymers because of its various coordination modes.[13] However, complexes based upon lanthanide SBUs and sulfates with H_3bidc have not been reported. Herein, we report the crystal structures, luminescence and magnetic properties of the novel lanthanide coordination polymers obtained by $Ln(NO_3)\cdot 6H_2O$, H_3bidc and KSCN under hydrothermal conditions. They are constructed from tetranuclear and dinuclear lanthanide SBUs with sulfate as the auxiliary bridge. The sulfates were *in situ* generated by oxidation of KSCN.

[a]*Department of Chemistry, College of Science, Shanghai University, Shanghai, 200444, P. R. China. E-mail: zxwang@shu.edu.cn; mx_li@mail.shu.edu.cn; Fax: +(86) 21 66132797*
[b]*Instrumental Analysis and Research Center, Shanghai University, Shanghai, 200444, P. R. China*
[c]*School of Chemistry and Materials Engineering, Wenzhou University, Wenzhou, 325027, P. R. China*

† Electronic supplementary information (ESI) available: X-ray crystallographic data in CIF format of complex **1–8**, selected bond lengths for **1**, **2**, **4**, **5**, **6**, and **8** (Tables S1 and S2), the luminescence of complexes **1**, **2**, **3**, **7**, and **8** in the solid state at room temperature (Fig. S1) and TGA for these complexes (Fig. S2). CCDC reference numbers 734649–734656 for complexes **1–8**. For ESI and crystallographic data in CIF or other electronic format see DOI: 10.1039/b910701k

Experimental

All chemicals are analytical grade and used as purchased without further purification. Elemental analyses for carbon, hydrogen, and nitrogen were carried out with a Vario EL III elemental analyzer. Infrared spectra were recorded with a Nicolet A370 FT-IR spectrometer using KBr pellets in the 4000–400 cm^{-1} region. TGA experiments were performed on a Shimadzu DT-20B thermogravimetric analyzer from 20 to 800 °C at a heating rate of 10 °C min^{-1} in nitrogen. The luminescence spectra were measured on a Shimadzu RF-5301 spectrophotometer. Variable-temperature magnetic susceptibility measurements were taken at an applied field of 100 Oe on a Quantum Design MPMS-XL7 SQUID magnetometer working in the temperature range of 300–1.8 K. The molar magnetic susceptibilities were corrected for the diamagnetism estimated from Pascal's tables and for the sample holder by previous calibration.

Preparation of $[La_2(Hbidc)_2(SO_4)(H_2O)_3]_n$ (1)

A mixture of $La(NO_3)_3\cdot 6H_2O$ (0.2 mmol), KSCN (0.1 mmol), H_3bidc (0.2 mmol), and water (10 mL) was sealed in a 15-mL Teflon-lined stainless-steel reactor, which was heated at 180 °C for 72 h under autogenous pressure. Upon cooling to room temperature at a rate of 10 °C h^{-1}, colorless sheet crystals suitable for X-ray diffraction were obtained with 74% yield based on La(III). Anal. Calcd (%) for $C_{18}H_{14}N_4O_{15}SLa_2$: C, 25.85; H, 1.69; N, 6.70. Found: C, 25.29; H, 1.83; N, 6.70. Selected IR data (KBr, cm^{-1}): 3578w, 3451s, 3062w, 1649w, 1629w, 1589s, 1543vs, 1471s, 1414vs, 1347w, 1214s, 1144s, 1044s, 810w, 786w, 632w.

Preparation of $[Pr_2(Hbidc)_2(SO_4)(H_2O)_3]_n$ (2)

This compound was synthesized with a similar procedure as described for synthesis of **1**, except $Pr(NO_3)_3\cdot 6H_2O$ used instead of $La(NO_3)_3\cdot 6H_2O$. Colorless sheet crystals were obtained with 12% yield based on Pr(III). Anal. Calcd (%) for $C_{18}H_{14}N_4O_{15}SPr_2$: C, 25.73; H, 1.68; N, 6.67. Found: C, 25.41; H, 1.73; N, 6.62. Selected IR data (KBr, cm^{-1}): 3582w, 3449s, 3063w, 1649w, 1627w, 1587s, 1537vs, 1472s, 1417vs, 1346w, 1213s, 1145s, 1047s, 809w, 785w, 632w.

Preparation of $[Sm_2(Hbidc)_2(SO_4)(H_2O)_3]_n$ (3)

This compound was synthesized with a similar procedure as described for synthesis of **1**, except $Sm(NO_3)_3\cdot 6H_2O$ used instead of $La(NO_3)_3\cdot 6H_2O$. Light yellow sheet crystals were obtained with 11% yield based on Sm(III). Anal. Calcd (%) for $C_{18}H_{14}N_4O_{15}SSm_2$: C, 25.16; H, 1.64; N, 6.52. Found: C, 23.90; H, 1.67; N, 7.46. Selected IR data (KBr, cm^{-1}): 3585s, 3451s, 3067w, 1650w, 1628w, 1588s, 1549vs, 1473s, 1421vs, 1348w, 1214s, 1151s, 1051s, 812w, 788w, 632w.

Preparation of $[Gd_2(Hbidc)_2(SO_4)(H_2O)_3]_n$ (4)

This compound was synthesized with a similar procedure as described for synthesis of **1**, except $Gd(NO_3)_3\cdot 6H_2O$ used instead of $La(NO_3)_3\cdot 6H_2O$. Colorless block crystals were obtained with 34% yield based on Gd(III). Anal. Calcd (%) for $C_{18}H_{14}N_4O_{15}SGd_2$: C, 24.77; H, 1.62; N, 6.42. Found: C, 25.13; H, 1.47; N, 6.56. Selected IR data (KBr, cm^{-1}): 3585s, 3450s, 3067w, 1653w, 1629w, 1588s, 1551vs, 1473s, 1423vs, 1349w, 1213s, 1152s, 1055s, 813w, 788w, 633w.

Preparation of $[Eu_4(Hbidc)_4(SO_4)_2]_n\cdot 2nH_2O$ (5)

This compound was synthesized with a similar procedure as described for the synthesis of **1**, except $Eu(NO_3)_3\cdot 6H_2O$ used instead of $La(NO_3)_3\cdot 6H_2O$. Colorless block crystals were obtained with 22% yield based on Eu(III). Anal. Calcd (%) for $C_{36}H_{20}N_8O_{26}S_2Eu_4$: C, 26.16; H, 1.22; N, 6.78. Found: C, 25.70; H, 1.53; N, 6.59. Selected IR data (KBr, cm^{-1}): 3570w, 3457s, 3338s, 3119s, 1643w, 1602s, 1573s, 1548s, 1508s, 1465s, 1399vs, 1368s, 1163s, 1116s, 1063s, 830w, 781w, 627w.

Preparation of $[Tb_4(Hbidc)_4(SO_4)_2]_n\cdot 2nH_2O$ (6)

This compound was synthesized with a similar procedure as described for the synthesis of **1**, except $Tb(NO_3)_3\cdot 6H_2O$ used instead of $La(NO_3)_3\cdot 6H_2O$. Colorless cubic crystals were obtained with 35% yield based on Tb(III). Anal. Calcd (%) for $C_{36}H_{20}N_8O_{26}S_2Tb_4$: C, 25.73; H, 1.20; N, 6.67. Found: C, 24.98; H, 1.41; N, 6.57. Selected IR data (KBr, cm^{-1}): 3568w, 3459w, 3326w, 3119s, 1605s, 1574s, 1550s, 1510s, 1467s, 1399vs, 1370s, 1156s, 1115s, 1065s, 831w, 781w, 627w.

Preparation of $[Dy_4(Hbidc)_4(SO_4)_2]_n\cdot 2nH_2O$ (7)

This compound was synthesized with a similar procedure as described for the synthesis of **1**, except $Dy(NO_3)_3\cdot 6H_2O$ was used instead of $La(NO_3)_3\cdot 6H_2O$. Colorless cubic crystals were obtained with 37% yield based on Dy(III). Anal. Calcd (%) for $C_{36}H_{20}N_8O_{26}S_2Dy_4$: C, 25.51; H, 1.19; N, 6.61. Found: C, 24.88; H, 1.41; N, 6.43. Selected IR data (KBr, cm^{-1}): 3570s, 3459s, 3316s, 3119s, 1638w, 1606s, 1574s, 1551s, 1511s, 1468s, 1402vs, 1371s, 1163s, 1117s, 1064s, 832w, 780w, 627w.

Preparation of $[Er_4(Hbidc)_4(SO_4)_2]_n\cdot 2nH_2O$ (8)

This compound was synthesized with a similar procedure as described for synthesis of **1**, except $Er(NO_3)_3\cdot 6H_2O$ used instead of $La(NO_3)_3\cdot 6H_2O$. Pink block crystals were obtained with 21% yield based on Er(III). Anal. Calcd (%) for $C_{36}H_{20}N_8O_{26}S_2Er_4$: C, 25.23; H, 1.18; N, 6.54. Found: C, 24.66; H, 1.42; N, 6.43. Selected IR data (KBr, cm^{-1}): 3570w, 3458s, 3120w, 1639w, 1608s, 1574s, 1554s, 1512s, 1470s, 1404vs, 1372s, 1161s, 1119s, 1064s, 833w, 780w, 629w.

X-ray crystallography

The crystal data for complexes **1–8** were collected on a Bruker Smart Apex-II CCD diffractometer at room temperature. Intensities were collected with graphite monochromatized Mo-Kα radiation (λ = 0.71073 Å), using the φ and ω scan technique. The data reduction was made with the SAINT package. Absorption corrections were performed using the SADABS program. The structures were solved by direct methods and refined on F^2 by full-matrix least-squares using the SHELXTL-2000 program package with anisotropic displacement parameters for all non-hydrogen atoms.[14] Hydrogen atoms

Table 1 Crystallographic data for **1–4**

Complexes	**1**	**2**	**3**	**4**
Formula	$C_{18}H_{14}N_4O_{15}SLa_2$	$C_{18}H_{14}N_4O_{15}SPr_2$	$C_{18}H_{14}N_4O_{15}SSm_2$	$C_{18}H_{14}N_4O_{15}SGd_2$
Formula weight	836.21	840.21	859.12	872.89
Crystal system	Triclinic	Triclinic	Triclinic	Triclinic
Space group	$P\bar{1}$	$P\bar{1}$	$P\bar{1}$	$P\bar{1}$
a/Å	9.6550(17)	9.5697(13)	9.4730(11)	9.4361(15)
b/Å	10.0259(18)	9.9532(13)	9.8689(11)	9.8459(15)
c/Å	14.313(3)	14.288(2)	14.2483(16)	14.246(2)
α (°)	91.012(2)	91.200(2)	91.4250(10)	91.443(2)
β (°)	107.625(2)	107.652(2)	107.6770(10)	107.665(2)
γ (°)	118.626(2)	118.4730(10)	118.2570(10)	118.251(2)
V/Å^3	1136.9(4)	1117.5(3)	1095.1(2)	1088.2(3)
Z	2	2	2	2
Dc (g cm^{-3})	2.443	2.497	2.605	2.664
μ/mm^{-1}	3.890	4.495	5.500	6.233
F(000)	800	808	820	828
Reflections collected/unique	5858/3919	5823/3926	5906/3992	5873/3954
Data/restraints/parameters	3919/6/367	3926/6/361	3992/0/361	3954/0/361
GOF (F^2)	1.232	1.010	1.149	1.083
$R_1{}^a[I > 2\sigma(I)]$	0.0537	0.0425	0.0272	0.0304
$wR_2{}^b[I > 2\sigma(I)]$	0.1336	0.0990	0.0730	0.0748

^{a} $R_1 = \sum||F_o| - |F_c||/\sum|F_o|$. ^{b} $wR_2 = [\sum w(|F_o^2| - |F_c^2|)^2/\sum w(|F_o^2|)^2]^{1/2}$.

Table 2 Crystallographic data for **5–8**

Complexes	**5**	**6**	**7**	**8**
Formula	$C_{36}H_{20}N_8O_{26}S_2Eu_4$	$C_{36}H_{20}N_8O_{26}S_2Tb_4$	$C_{36}H_{20}N_8O_{26}S_2Dy_4$	$C_{36}H_{20}N_8O_{26}S_2Er_4$
Formula weight	1652.62	1680.40	1694.72	1713.76
Crystal system	Monoclinic	Monoclinic	Monoclinic	Monoclinic
Space group	$P\ 2_1/c$	$P\ 2_1/c$	$P\ 2_1/c$	$P\ 2_1/c$
a/Å	9.5378(8)	9.5378(8)	9.5378(8)	9.5378(8)
b/Å	6.6828(5)	6.6828(5)	6.6828(5)	6.6828(5)
c/Å	16.1310(13)	16.1310(13)	16.1310(13)	16.1310(13)
β (°)	96.7490(10)	96.7490(10)	96.7490(10)	96.7490(10)
V/Å^3	1021.05(14)	1021.05(14)	1021.05(14)	1021.05(14)
Z	1	1	1	1
Dc (g cm^{-3})	2.688	2.733	2.756	2.787
μ/mm^{-1}	6.277	7.061	7.452	8.353
F(000)	784	792	796	804
Reflections collected/unique	5294/1878	5104/1805	5263/1876	4829/1810
Data/restraints/parameters	1878/0/190	1805/0/190	1876/0/190	1810/24/190
GOF (F^2)	1.185	1.152	1.177	1.176
$R_1{}^a[I > 2\sigma(I)]$	0.0533	0.0541	0.0445	0.0512
$wR_2{}^b[I > 2\sigma(I)]$	0.1220	0.1232	0.1078	0.1347

^{a} $R_1 = \sum||F_o| - |F_c||/\sum|F_o|$. ^{b} $wR_2 = [\sum w(|F_o^2| - |F_c^2|)^2/\sum w(|F_o^2|)^2]^{1/2}$.

were introduced in calculations using the riding model. The crystal data and structural refinement results are summarized in Tables 1 and 2.

Results and discussion

Preparations and infrared spectra

The complexes **1–8** were obtained by hydrothermal reactions of $Ln(NO_3)\cdot 6H_2O$ with KSCN and H_3bidc. The sulfate anions were *in situ* generated by oxidation of KSCN during the reaction.[7f] In order to confirm the sulfate anions, we identified the following experimental phenomena: (1) the colorless residual solution has a characteristically pungent smell, which indicates production of H_2S in the reactions; (2) white $BaSO_4$ precipitate, produced immediately by addition of a $BaCl_2$ solution into the filtrate, was not dissolved in dilute HNO_3. No precipitate was observed by addition of $BaCl_2$ to the mixture of reacting reagent. Lanthanide metals are used as catalysts in a wide variety of organic transformations, also in the catalytic oxidation of sulfides.[15] About the mechanism for the transformation of SCN^- into SO_4^{2-}, we assume that sulfate is generated by the dismutation reaction of S with H_2O under the catalysis of lanthanide ions. Sulfur derives from the decomposition of SCN^- under the present reaction conditions.[16] Interestingly, when K_2SO_4 instead of KSCN was introduced directly into the reacting mixture, the target products were not obtained.

Infrared spectra of **1–8** show characteristic bands of sulfate in the region from 1265 to 920 cm^{-1}. The characteristic absorptions of sulfate in 1065–1044 cm^{-1} and 1214–1115 cm^{-1} respectively indicate that bridge bidentate and chelating bidentate coordination modes are adopted,[17] which are in agreement with the crystal structures of **1–8**. All carboxyl groups of H_3bidc in **1–8** are deprotonated, according to IR spectra in which no absorption peaks occur near 1700 cm^{-1} for –COOH. The strong peaks are around 1590–1413 cm^{-1} for **1–4** and 1643–1399 cm^{-1} for **5–8**, which is characteristic for expected absorption of asymmetric and symmetric vibrations of carboxylate groups. In addition, N–H absorption of imidazole appears at about 3450 cm^{-1}.

Crystal structures of 1–4

X-ray crystallgraphy reveals that complexes **1–4** are isomorphous, which crystallize in the triclinic $P\bar{1}$ space group and comprise 2D metal–organic frameworks based upon square-planar tetranuclear lanthanide SBUs. Thus we will restrict our presentation and discussion on the structure of the samarium complex. A view of the asymmetric unit of **3** with atom labeling is illustrated in Fig. 1. The unit contains two crystallographically independent samarium ions, two $Hbidc^{2-}$ dianions, one sulfate, and three coordinated water molecules. The Sm1 is eight-coordinated

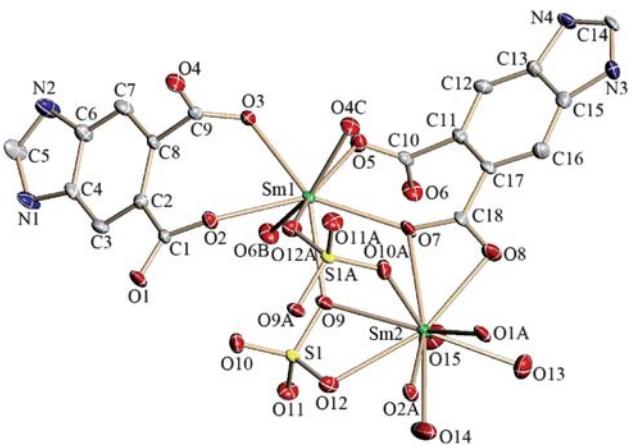

Fig. 1 View of the asymmetric unit of **3** showing ellipsoids at the 50% probability level. Hydrogen atoms are omitted for clarity.

Table 3 Selected bond distances (Å) for **3**[a]

Sm1–O2	2.460(3)	Sm1–O3	2.395(3)
Sm1–O4[c]	2.397(3)	Sm1–O5	2.385(3)
Sm1–O6[b]	2.336(3)	Sm1–O7	2.444(3)
Sm1–O9	2.512(3)	Sm1–O12[a]	2.470(3)
Sm2–O1[a]	2.585(3)	Sm2–O2[a]	2.513(3)
Sm2–O7	2.659(3)	Sm2–O8	2.436(3)
Sm2–O9	2.636(3)	Sm2–O10[a]	2.402(3)
Sm2–O12	2.588(4)	Sm2–O13	2.494(4)
Sm2–O14	2.462(4)	Sm2–O15	2.471(4)

[a] Symmetry transformation used to generate equivalent atoms: a: −x + 1, −y + 2, −z; b: −x, −y + 1, −z; c: −x + 1, −y + 1, −z.

and involved in a distorted square antiprism geometry bound to six carboxylate oxygen atoms (O2, O3, O4C, O5, O6B, O7) from four $Hbidc^{2-}$, and two oxygen atoms (O9, O12A) from two SO_4^{2-}. In the distorted square antiprism, O2, O3, O4C, and O12A are situated on the four sites in a square plane with a mean deviation of 0.0188 Å and the other oxygen atoms O5, O7, O6B, and O9 in another square plane with a mean deviation of 0.1035 Å. Compared to Sm1, Sm2 is ten-coordinated with four carboxylate oxygen atoms (O1A, O2A, O7, O8) from two $Hbidc^{2-}$, and three oxygen atoms (O9, O10A, O12) from two SO_4^{2-}. The remaining three coordinate sites are occupied by coordinated water molecules. The Sm–O bond lengths range from 2.336(3) to 2.636(3) Å (Table 3), which are expected as those observed in reported Sm(III) complexes.[12b]

Both $Hbidc^{2-}$ ligands in the asymmetric unit adopt the same coordination mode as depicted in Scheme 1a. Each $Hbidc^{2-}$ ligand acts as a μ_3-bridge and connects three Sm(III) *via* four oxygen atoms belonging to two different carboxyl groups (O1/O2, O2/O4, and O3; O5, O6/O7, and O7/O8). Sm1 links two neighboring Sm2 by O2 and O7 to form a square-planar tetranuclear samarium (Sm_4) SBU as given in Fig. 2. In the SBU, the Sm1···Sm2 distances are 4.288 and 4.232 Å, respectively. Each sulfate anion provides two μ_2-O atoms (O9 and O12) to bridge three Sm ions of the Sm_4 SBU and the third oxygen atom (O10) binding to the remainder (Scheme 1c). The fourth oxygen atom of the SO_4^{2-} anion is free but involved in formation of hydrogen bonds. Therefore, the Sm_4 SBU was strengthened by two sulfate anions serving as "splints". Furthermore, each SBU connects four neighboring SBUs by two double O3–C9–O4 and O5–C10–O6 bridges, which leads to a 2D layer in the *ab* plane showing a topology with Schläfli symbol $(3^2{\cdot}4^2{\cdot}5^2)$[18] as node of Sm_4 (Fig. 3). In the solid state, the 2D layers extend to a three-dimensional network by cooperative interactions of π–π

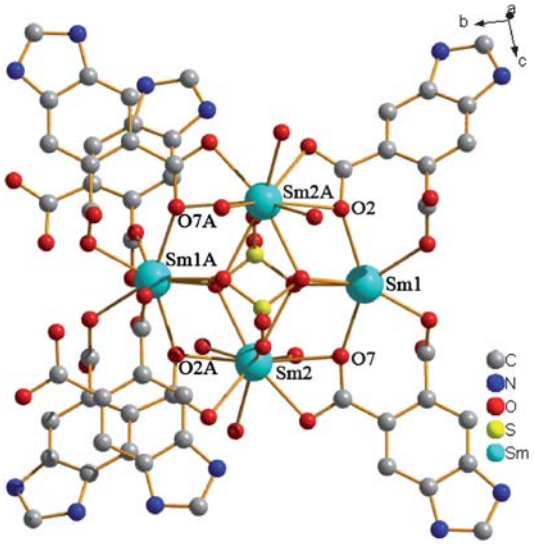

Fig. 2 Projection of the Sm_4 SBU. Hydrogen atoms are omitted for clarity.

stacking of the imidazole rings and hydrogen bonding which is shown in Fig. 4.

Crystal structures of 5–8

Complexes **5–8** are isomorphous with each other, which crystallize in the monoclinic $P2_1/c$ space group and contain interesting 3D metal–organic frameworks based on dinuclear lanthanide SBUs linked by $Hbidc^{2-}$ and SO_4^{2-} anions. The crystal structure of **7** is described in detail. The asymmetric unit comprises one Dy(III) ion, one $Hbidc^{2-}$, and half SO_4^{2-} anion (Fig. 5). The Dy(III) ion is eight-coordinate with five carboxylate oxygen atoms (O1, O2, O2A, O3A, O4B) from three $Hbidc^{2-}$, two oxygen atoms (O5, O6A) from two SO_4^{2-}, and one nitrogen atom (N1C) from $Hbidc^{2-}$. The Dy–O bond lengths are in the range of 2.216(7) Å to 2.524(8) Å, and the Dy–N bond length is 2.526(9) Å (Table 4). The $Hbidc^{2-}$ ligand showing a μ_4-bridge (Scheme 1b) which is observed in $\{[Tb(L)(HL)(H_2O)]\cdot H_2O\}_n$ ($L = Hbidc^{2-}$),[11] connects four Dy(III) *via* one nitrogen and four oxygen atoms (N1, O1, O2, O3, O4). The SO_4^{2-} anion with positional disorder in the structure provides three oxygen atoms to bridge three Dy(III) ions (Scheme 1d).

Two adjacent Dy(III) ions are bridged by μ-O2 atoms to form Dy_2 dinuclear SBU, which is presented in Fig. 6. Interestingly, these Dy_2 SBUs are connected by sulfate bridges to produce a 1D

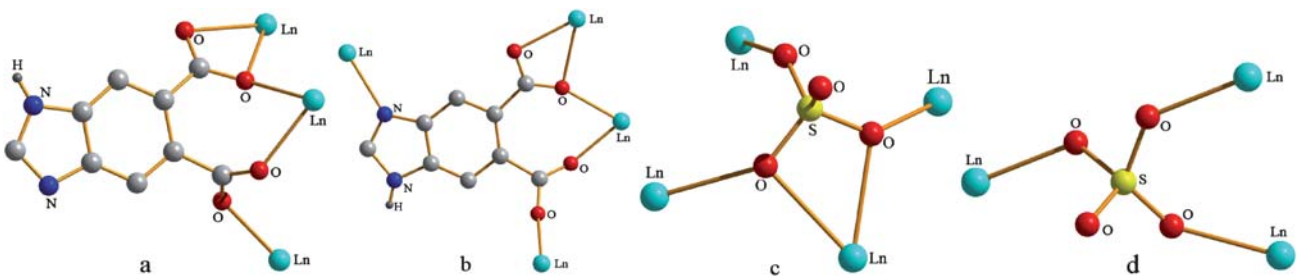

Scheme 1 Coordination modes of the $Hbidc^{2-}$and SO_4^{2-} anions.

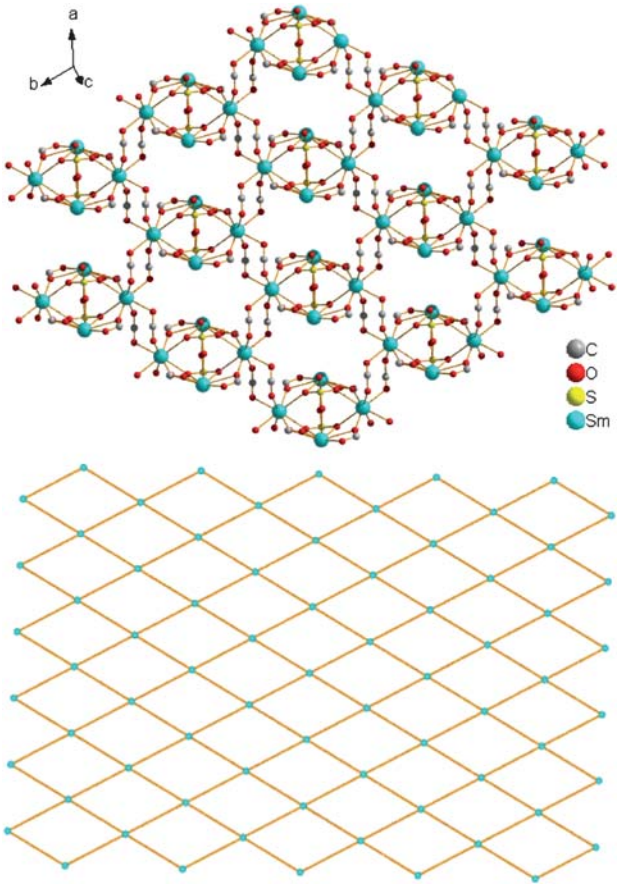

Fig. 3 2D layer constructed from Sm_4 SBUs (top), and the topology showing the connectivity between Sm_4 nodes (sky blue spheres) (bottom). Non-bridging atoms of ligands and hydrogen atoms have been omitted for clarity.

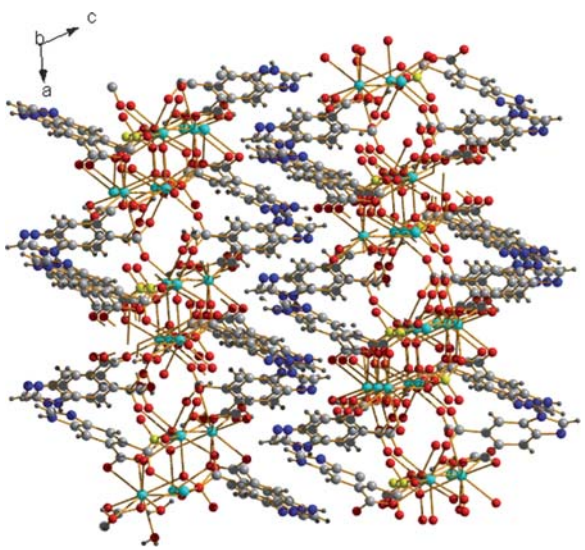

Fig. 4 3D supramolecular framework of **3** formed by cooperative interactions of π–π stacking of the imidazole rings and hydrogen bonding.

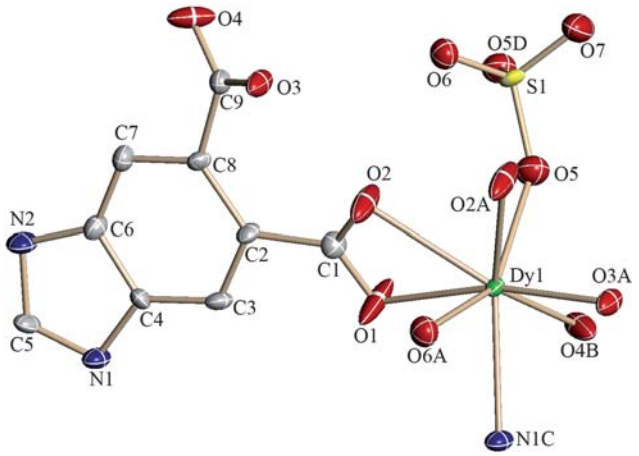

Fig. 5 Coordination environment of Dy atom with the thermal ellipsoids draw at 50% probability level. Hydrogen atoms, lattice water, and the second disorder position of O7 and S1 from SO_4^{2-} are omitted for clarity.

Table 4 Selected bond distances (Å) and angles (deg) for **7**[a]

Dy1–O1	2.374(9)	Dy1–O2	2.524(8)
Dy1–O2[a]	2.355(8)	Dy1–O3[a]	2.216(7)
Dy1–O4[b]	2.296(8)	Dy1–O5	2.335(18)
Dy1–O6[a]	2.353(8)	Dy1–N1[c]	2.526(9)

[a] Symmetry transformation used to generate equivalent atoms: a: −x + 1, −y + 1, −z + 1; b: x, −y + 1/2, z−1/2; c: −x + 2, −y + 1, −z + 1.

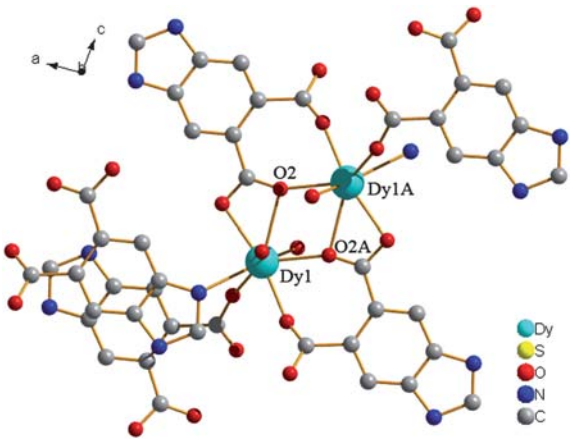

Fig. 6 The structure of dinuclear Dy_2 SBU. Hydrogen atoms are omitted for clarity.

Dy_2–sulfate chain along the *b* axis (Fig. 7). Each chain is linked to eight adjacent and parallel chains by $Hbidc^{2-}$ through carboxylate and imidazole groups to generate a 3D structure (Fig. 8). The non-coordinated water molecules are stabilized in the lattice by hydrogen bonds.

Through the structure formation of these complexes, the effect of lanthanide contraction was observed. In **5–8**, the metal centers are only eight-coordinate, while metal centers which are ten-coordinate are found in complexes **1–4**. Moreover, the contraction effects on the family of complexes are also reflected in the

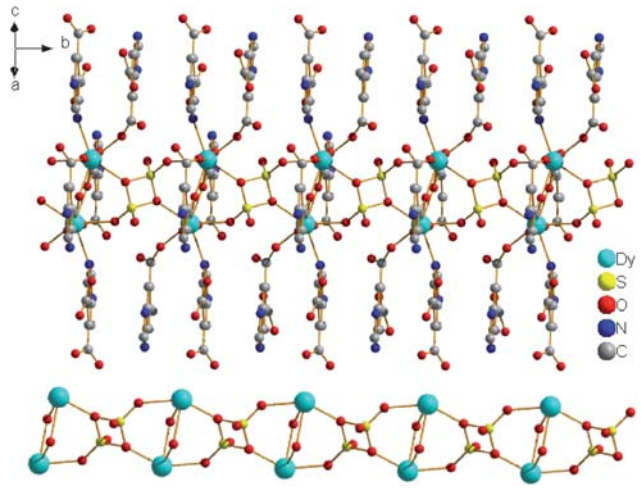

Fig. 7 1D chain based on sulfate bridging Dy_2 SBUs along the *b* direction (top), the core of the 1D chain (bottom), sulfate is disordered.

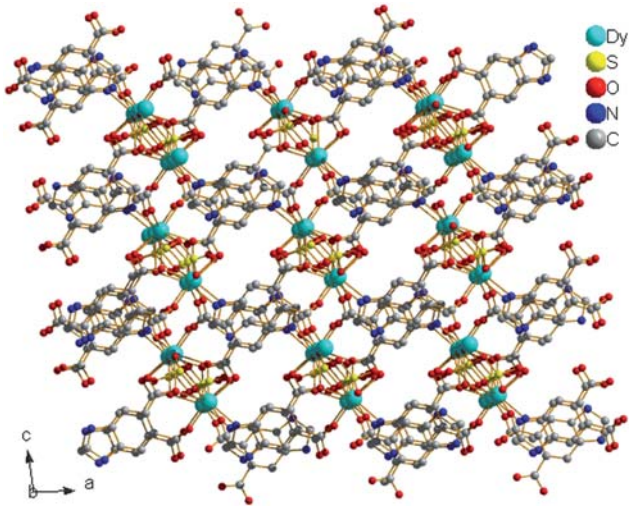

Fig. 8 Packing diagram of **7** along the *b* axis, guest water molecules are omitted.

Ln–O bond lengths. It is interesting that the elements Eu and Gd give rise to a location swap. As a result, we guess that both kinds of structures would exist for elements Eu and Gd.

Luminescence properties and thermogravimetric analyses

The luminescent spectra of **1–8** in the solid state were recorded at room temperature. Because the energy gap of the lanthanide ions (Pr^{3+}, Sm^{3+}, Dy^{3+}, Er^{3+}) is quite large and La(III) has no *f–f* transition, the luminescence of **1**, **2**, **3**, **7**, and **8** originates from the ligand H_3bidc (ESI, Fig. S1†). Fig. 9 presents the emission spectra of the complexes **4**, **5**, and **6**. Upon excitation at 355 nm, complex **4** shows a broadband emission in the range 400–650 nm, which was also observed in other Gd^{3+} complexes.[20] Compared to the strongest wavelength (λ_{max} = 389 nm) of the free H_3bidc ligand, the λ_{max} of complex **4** located at 498 nm is clearly red-shifted. Generally, the emission spectra of Gd(III) complexes occur out of the visible region, due to a highly energetic

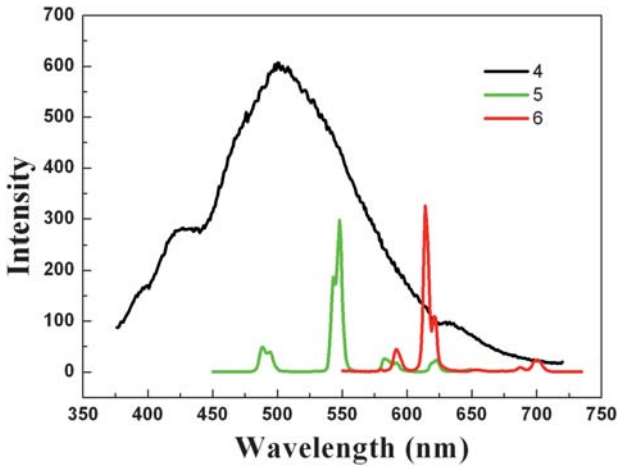

Fig. 9 Solid-state emission spectra of **4**, **5**, and **6** at room temperature.

difference between the first excited state of Gd^{3+} and the fundamental levels.[21] Therefore, the strong emission of **4** probably involves ligand-to-metal charge transfer, formed by the orbital overlap of the ligand and Gd^{3+} energy levels.[20]

For the complex **5**, irradiated at 537 nm, the characteristic emissions of Eu(III) are obtained distinctly at 592, 614, and 700 nm, corresponding to $^5D_0 \rightarrow {}^7F_1$, $^5D_0 \rightarrow {}^7F_2$, and $^5D_0 \rightarrow {}^7F_4$ transitions. It is well known that the $^5D_0 \rightarrow {}^7F_1$ transition is magnetic dipole in nature and less sensitive to its environment, while $^5D_0 \rightarrow {}^7F_2$ is electric dipole in origin and its intensity is strongly influenced by the crystal field.[22] The comparable intensities of $^5D_0 \rightarrow {}^7F_1$ and $^5D_0 \rightarrow {}^7F_2$ transitions imply relatively low-symmetric crystal field for the center metal of Eu(III) in **5**, according with the single-crystal structure.

The luminescence spectrum collected for complex **6** also shows the characteristic emission of Tb(III) which is impressive as all the transitions to the ground-state manifold are from the emitting $^5D_4$ level, assigned to $^5D_4 \rightarrow {}^7F_J$ (J = 3, 4, 5, 6), $^5D_4 \rightarrow {}^7F_6$ (488 nm), $^5D_4 \rightarrow {}^7F_5$ (548 nm), $^5D_4 \rightarrow {}^7F_4$ (583 nm), and $^5D_4 \rightarrow {}^7F_3$ (623 nm) transitions. The $^5D_4 \rightarrow {}^7F_5$ is the most intense transition showing strong green light and consisting of an intense band with one weak shoulder at higher frequency. The others are less intense broad peaks with small shoulders at lower frequency. This luminescent phenomenon was observed in terbium complexes.[23]

The thermal stabilities of complexes **1–8** were investigated through thermogravimetric experiments. The isomorphous complexes **1–4** and **5–8** show two types of TG curves (ESI, Fig. S2†). Only **1** and **5** are selected for description. Both complexes are stable until 250 °C, and then a gradual weight-loss process was observed. The rapid weight-loss process started at *ca.* 390 °C for **1** and 470 °C for **5**, corresponding to the decomposition of organic ligand. Considering the high thermal stability of sulfate, the final residues are $La_2O_2SO_4$ (found 48.74%, calc. 48.54%) and $Eu_2O_2SO_4$ (found 51.85%, calc. 52.28%), respectively.

Magnetic properties

Variable-temperature magnetic susceptibility measurements were carried out on crystalline samples of **4** and **6–8** at an applied

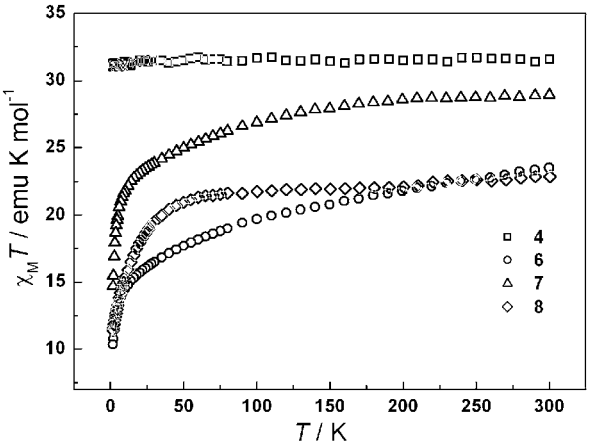

Fig. 10 Temperature dependence of magnetic susceptibilities of **4** and **6–8** in an applied field of 100 Oe.

magnetic field of 100 Oe in the temperature range of 1.8–300 K. The plots of $\chi_m T$ *versus* T are shown in Fig. 10, where $\chi_m T$ is the corrected molar magnetic susceptibility per Ln_4 unit for complex **4** and Ln_2 unit for complexes **6–8**. For complex **4**, $\chi_m T$ is almost a constant of 31.58 cm^3 K mol^{-1} in the investigated temperature range, which is closest to the calculated value, 31.52 cm^3 K mol^{-1}, considering the contribution of four uncoupled Gd(III) ions (7.88 cm^3 K mol^{-1}, expected value).[24] The magnetic property indicates that there is very weak magnetic interaction between the metal centers even though it is negligible. This paramagnetic behavior was reported in the literature for the Gd(III) compounds, probably due to the Gd(III) centers showing a $4f^7$ electron configuration with no orbital degeneracy.[25]

In the case of complexes **6–8**, they display similar magnetic properties due to their isomorphosity. Compared to the magnetic behavior of **4**, the magnetic properties of **6–8** are more complicated because of the existence of the spin–orbit coupling of Ln(III) ions. As can be seen from Fig. 10, the $\chi_m T$ are 23.31, 28.62, and 22.72 cm^3 K mol^{-1} at room temperature for **6–8**, respectively, which are very close to the calculated values, 23.64, 28.34, and 22.96 cm^3 K mol^{-1} for the contributions of dinuclear uncoupled Tb(III) (11. 28 cm^3 K mol^{-1}, expected value), Dy(III) (14.17 cm^3 K mol^{-1}), and Er(III) (11.48 cm^3 K mol^{-1}).[24] Upon cooling the system, $\chi_M T$ continuously decreases over the whole temperature range and reaches 10.34, 14.68, and 11.39 emu K mol^{-1} at 1.8 K comparable with the results reported previously,[5d,26] indicating that the magnetic susceptibility deviates from the Curie law because of the thermal depopulation of Stark levels. The thermal depopulation of the Stark sublevels originated from the splitting of the free-ion ground state in the Ln(III) ion. Therefore, the nature of the magnetic interactions between the lanthanide metal ions cannot be determined only from the features of the $\chi_m T$–T curves. Usually, the couplings involving Ln(III) ions are very weak and are not directly deduced from the temperature dependence of the magnetic susceptibility owing to strong spin–orbit coupling.

Conclusions

This work demonstrates eight novel lanthanide coordination polymers obtained by $Ln(NO_3)\cdot 6H_2O$, H_3bidc and KSCN under hydrothermal conditions. They are constructed from tetranuclear and dinuclear lanthanide SBUs with sulfate as auxiliary bridge. The sulfates were *in situ* generated by catalytic oxidation of KSCN. The structures of **1–8** involve the interesting feature that the frameworks are formed from lanthanide SBUs and H_3bidc carboxylate bridges. **1–4** are isomorphous with one another and comprise 2D frameworks based upon square-planar tetranuclear lanthanide SBUs, while **5–8** are also isomorphous and display 3D networks fabricated through $Hbidc^{2-}$ and SO_4^{2-} bridging dinuclear lanthanide SBUs. The complexes **5** and **6** exhibit characteristic europium and terbium luminescence, while **4** involves ligand-to-metal charge transfer. The magnetic properties of four complexes have been investigated in detail. Due to strong spin–orbit coupling, **6–8** present lanthanide(III) ion magnetism, whereas **4** without orbital degeneracy shows paramagnetic behavior.

Acknowledgements

This work was supported by the National Natural Science Foundation of China (20901049), the Leading Academic Discipline Project of Shanghai Municipal Education Commission (J50102), the Excellent Youth Teachers Foundation of Shanghai Municipal Education Commission, and the Innovation Foundation of Shanghai University.

References

1 (*a*) M. Eddaoudi, D. B. Moler, H. Li, B. Chen, T. M. Reineke, M. O'Keeffe and O. M. Yaghi, *Acc. Chem. Res.*, 2001, **34**, 319; (*b*) N. W. Ockwig, O. Delgado-Friedrichs, M. O'Keeffe and O. M. Yaghi, *Acc. Chem. Res.*, 2005, **38**, 176; (*c*) R.-Q. Zou, H. Sakurai, S. Han, R.-Q. Zhong and Q. Xu, *J. Am. Chem. Soc.*, 2007, **129**, 8402; (*d*) L. F. Jones, A. Prescimone, M. Evangelisti and E. K. Brechin, *Chem. Commun.*, 2009, 2023.

2 (*a*) J. Yoo, W. Wernsdorfer, E.-C. Yang, M. Nakano, A. L. Rheigold and D. N. Hendrickson, *Inorg. Chem.*, 2005, **44**, 3377; (*b*) T. E. Vos and J. S. Miller, *Angew. Chem., Int. Ed.*, 2005, **44**, 2416; (*c*) A. J. Cairns, J. A. Perman, L. Wojtas, V. Ch. Kravtsov, M. H. Alkordi, M. Eddaoudi and M. J. Zaworotko, *J. Am. Chem. Soc.*, 2008, **130**, 1560; (*d*) F. Nouar, J. F. Eubank, T. Bousquet, L. Wojtas, M. J. Zaworotko and M. Eddaoudi, *J. Am. Chem. Soc.*, 2008, **130**, 1833.

3 (*a*) M. Dinca, A. Dailly, Y. Liu, C. M. Brown, D. A. Neumann and J. R. Long, *J. Am. Chem. Soc.*, 2006, **128**, 16876; (*b*) X. Lin, J. H. Jia, X. B. Zhao, K. M. Thomas, A. J. Blake, G. S. Walker, N. R. Champness, P. Hubberstey and M. Schröder, *Angew. Chem., Int. Ed.*, 2006, **45**, 7358; (*c*) S. Ma, J. Eckert, P. Forster, J. Yoon, Y. K. Hwang, J.-S. Chang, C. D. Collier, J. B. Parise and H.-C. Zhou, *J. Am. Chem. Soc.*, 2008, **130**, 15896; (*d*) Y.-L. Bai, J. Tao, R.-B. Huang and L.-S. Zheng, *Angew. Chem., Int. Ed.*, 2008, **47**, 5344.

4 (*a*) Z.-X. Wang, X.-F. Shen, J. Wang, P. Zhang, Y.-Z. Li, E. N. Nfor, Y. Song, S. Ohkoshi, K. Hashimoto and X.-Z. You, *Angew. Chem., Int. Ed.*, 2006, **45**, 3287; (*b*) S. Ma, D. Yuan, X.-S. Wang and H.-C. Zhou, *Inorg. Chem.*, 2009, **48**, 2072.

5 (*a*) X.-J. Zheng, L.-P. Jin and S. Gao, *Inorg. Chem.*, 2004, **43**, 1600; (*b*) D. Weng, X. Zheng and L. Jin, *Eur. J. Inorg. Chem.*, 2006, 4184; (*c*) A. Thirumurugan and S. Natarajan, *Cryst. Growth Des.*, 2006, **6**, 983; (*d*) Y.-G. Huang, B.-L. Wu, D.-Q. Yuan, Y.-Q. Xu, F.-L. Jiang and M.-C. Hong, *Inorg. Chem.*, 2007, **46**, 1171.

6 (*a*) M. Eddaoudi, J. Kim, J. B. Wachter, H. K. Chae, M. O'Keeffe and O. M. Yaghi, *J. Am. Chem. Soc.*, 2001, **123**, 4368; (*b*) Q.-R. Fang, G.-S. Zhu, M. Xue, Q.-L. Zhang, J.-Y. Sun, X.-D. Guo, S.-L. Qiu, S.-T. Xu, P. Wang, D.-J. Wang and Y. Wei, *Chem.–Eur. J.*, 2006, **12**, 3754; (*c*) Q.-R. Fang, G.-S. Zhu, Z. Jin, M. Xue, X. Wei, D.-J. Wang and S.-L. Qiu, *Angew. Chem., Int. Ed.*, 2006, **45**, 6126; (*d*) J. A. Rood, W. C. Boggess, B. C. Noll and K. W. Henderson,

J. Am. Chem. Soc., 2007, **129**, 13675; (*e*) Q.-G. Zhai, C.-Z. Lu, X.-Y. Wu and S. R. Batten, *Cryst. Growth Des.*, 2007, **7**, 2332; (*f*) H. Furukawa, J. Kim, N. W. Ockwig, M. O'Keeffe and O. M. Yaghi, *J. Am. Chem. Soc.*, 2008, **130**, 11650.

7 (*a*) C.-F. Wang, E.-Q. Gao, Z. He and C.-H. Yan, *Chem. Commun.*, 2004, 720; (*b*) Y. Liu, V. Kravtsov, R. D. Walsh, P. Poddar, H. Srikanth and M. Eddaoudi, *Chem. Commun.*, 2004, 2806; (*c*) Y.-Q. Sun, J. Zhang, Y.-M. Chen and G.-Y. Yang, *Angew. Chem., Int. Ed.*, 2005, **44**, 5814; (*d*) W.-G. Lu, C.-Y. Su, T.-B. Lu, L. Jiang and J.-M. Chen, *J. Am. Chem. Soc.*, 2006, **128**, 34; (*e*) Y. Wang, Y. Song, Z.-R. Pan, Y.-Z. Shen, Z. Hu, Z.-J. Guo and H.-G. Zheng, *Dalton Trans.*, 2008, 5588; (*f*) X.-H. Zhou, Y.-H. Peng, X.-D. Du, C.-F. Wang, J.-L. Zuo and X.-Z. You, *Cryst. Growth Des.*, 2009, **9**, 1028.

8 X.-M. Zhang, Z.-M. Hao, W.-X. Zhang and X.-M. Chen, *Angew. Chem., Int. Ed.*, 2007, **46**, 3456.

9 Y. Yao, Y. Che and J. Zheng, *Cryst. Growth Des.*, 2008, **8**, 2299.

10 (*a*) Y. L. Lo, W. C. Wang, G. A. Lee and Y. H. Liu, *Acta Crystallogr., Sect. E: Struct. Rep. Online*, 2007, **E63**, m2657; (*b*) Q. Gao, W.-H. Gao, C.-Y. Zhang and Y.-B. Xie, *Acta Crystallogr., Sect. E: Struct. Rep. Online*, 2008, **E64**, m928; (*c*) Y. Wei, Y. Yu and K. Wu, *Cryst. Growth Des.*, 2008, **8**, 2087; (*d*) Y. Wei, Y. Yu, R. Sa, Q. Li and K. Wu, *CrystEngComm*, 2009, **11**, 1054.

11 (*a*) C. R. Kagan, D. B. Mitzi and C. D. Dimitrakopoulos, *Science*, 1999, **286**, 945; (*b*) C. N. R. Rao, S. Natarajan, A. Choudhury, S. Neeraj and A. A. Ayi, *Acc. Chem. Res.*, 2001, **34**, 80; (*c*) J. N. Behera, G. Paul, A. Choudhury and C. N. R. Rao, *Chem. Commun.*, 2004, 456; (*d*) S. Ferrer, E. Aznar, F. Lloret, A. Castiñeiras, M. Liu-González and J. Borrás, *Inorg. Chem.*, 2007, **46**, 372; (*e*) F. Geng, Y. Matsushita, R. Ma, H. Xin, M. Tanaka, F. Izumi, N. Iyi and T. Sasaki, *J. Am. Chem. Soc.*, 2008, **130**, 16344.

12 (*a*) R. Vilar, D. M. P. Mingos, A. J. P. White and D. J. Williams, *Angew. Chem., Int. Ed.*, 1998, **37**, 1258; (*b*) Z. He, E.-Q. Gao, Z.-M. Wang, C.-H. Yan and M. Kurmoo, *Inorg. Chem.*, 2005, **44**, 862.

13 (*a*) D. Grohol, D. Papoutsakis and D. G. Nocera, *Angew. Chem., Int. Ed.*, 2001, **40**, 1519; (*b*) Y.-Q. Sun and G.-Y. Yang, *Dalton Trans.*, 2007, 3771; (*c*) Y. Lan, G. Novitchi, R. Clérac, J.-K. Tang, N. T. Madhu, I. J. Hewitt, C. E. Anson, S. Brooker and A. K. Powell, *Dalton Trans.*, 2009, 1721.

14 *Bruker, SMART, SAINT, SADABS and SHELXTL*, Bruker AXS Inc., Madison, WI, USA, 2000.

15 F. Gandara, J. Perles, N. Snejko, M. Iglesias, B. Gomez-Lor, E. Gutierrez-Puebla and M. A. Monge, *Angew. Chem., Int. Ed.*, 2006, **45**, 7998.

16 D. Li, T. Wu, X.-P. Zhou, R. Zhou and X.-C. Huang, *Angew. Chem., Int. Ed.*, 2005, **44**, 4175.

17 K. Nakamato, *Infrared and Raman Spectra of Inorganic and Coordination Compounds*, Wiley-Interscience: New York, 1978.

18 (*a*) A. F. Wells, *Three-dimensional Nets and Polyhedra*, Wiley: New York, 1977; (*b*) S. R. Batten and R. Robson, *Angew. Chem., Int. Ed.*, 1998, **37**, 1460.

19 J. A. Fernandes, R. A. Sá Ferreira, M. Pillinger, L. D. Carlos, I. S. Goncalves and P. J. A. Ribeiro-Claro, *Eur. J. Inorg. Chem.*, 2004, 3913.

20 (*a*) J. P. Leonard, C. B. Nolan, F. Stomeo and T. Gunnlaugsson, *Top. Curr. Chem.*, 2007, **281**, 1; (*b*) C.-H. Huang, *Rare Earth Coordination Chemistry*, Science Press: Beijing, 1997.

21 (*a*) A. F. Kirby, D. Foster and F. S. Richardson, *Chem. Phys. Lett.*, 1983, **95**, 507; (*b*) Q. Xu, L. Li, X. Liu and R. Xu, *Chem. Mater.*, 2002, **14**, 549; (*c*) Y. Kim, M. Suh and D.-Y. Jung, *Inorg. Chem.*, 2004, **43**, 245.

22 (*a*) S. Quici, M. Cavazzini, M. Marzanni, G. Accorsi, N. Armaroli, B. Ventura and F. Barigellett, *Inorg. Chem.*, 2005, **44**, 529; (*b*) Z.-H. Zhang, Y. Song, Y. Okamura, Y. Hasegawa, W.-Y. Sun and N. Ueyama, *Inorg. Chem.*, 2006, **45**, 2896; (*c*) F. Luo, Y. Che and J. Zheng, *Cryst. Growth Des.*, 2008, **8**, 2006; (*d*) M.-S. Liu, Q.-Y. Yu, Y.-P. Cai, C.-Y. Su, X.-M. Lin, X.-X. Zhou and J.-W. Cai, *Cryst. Growth Des.*, 2008, **8**, 4083.

23 (*a*) S. Raphael, M. L. P. Reddy, A. H. Cowley and M. Findlater, *Eur. J. Inorg. Chem.*, 2008, 4387; (*b*) X. Yang, R. A. Jones and W.-K. Wong, *Chem. Commun.*, 2008, 3266.

24 C. Benelli and D. Gatteschi, *Chem. Rev.*, 2002, **102**, 2369.

25 (*a*) H. Hou, G. Li, L. Li, Y. Zhu, X. Meng and Y. Fan, *Inorg. Chem.*, 2003, **42**, 428; (*b*) A. M. Atria, R. Baggio, M. T. Garland, J. C. Muñoz and O. Peña, *Inorg. Chim. Acta*, 2004, **357**, 1997.

26 (*a*) A. W.-H. Lam, W.-T. Wong, G. Wen, X.-X. Zhang and S. Gao, *New J. Chem.*, 2001, **25**, 531; (*b*) S.-N. Wang, R. Sun, X.-S. Wang, Y.-Z. Li, Y. Pan, J. Bai, M. Scheer and X.-Z. You, *CrystEngComm*, 2007, **9**, 1051; (*c*) L. Norel, L.-M. Chamoreau, Y. Journaux, O. Oms, G. Chastanet and C. Train, *Chem. Commun.*, 2009, 2381.

